Redox-Flow Batteries

International Edition: DOI: 10.1002/anie.201610582
German Edition: DOI: 10.1002/ange.201610582

Macromolecular Design Strategies for Preventing Active-Material Crossover in Non-Aqueous All-Organic Redox-Flow Batteries

*Sean E. Doris, Ashleigh L. Ward, Artem Baskin, Peter D. Frischmann, Nagarjuna Gavvalapalli, Etienne Chénard, Christo S. Sevov, David Prendergast, Jeffrey S. Moore, and Brett A. Helms**

Abstract: *Intermittent energy sources, including solar and wind, require scalable, low-cost, multi-hour energy storage solutions in order to be effectively incorporated into the grid. All-Organic non-aqueous redox-flow batteries offer a solution, but suffer from rapid capacity fade and low Coulombic efficiency due to the high permeability of redox-active species across the battery's membrane. Here we show that active-species crossover is arrested by scaling the membrane's pore size to molecular dimensions and in turn increasing the size of the active material above the membrane's pore-size exclusion limit. When oligomeric redox-active organics (RAOs) were paired with microporous polymer membranes, the rate of active-material crossover was reduced more than 9000-fold compared to traditional separators at minimal cost to ionic conductivity. This corresponds to an absolute rate of RAO crossover of less than 3 μmol cm^{-2} day^{-1} (for a 1.0 M concentration gradient), which exceeds performance targets recently set forth by the battery industry. This strategy was generalizable to both high and low-potential RAOs in a variety of non-aqueous electrolytes, highlighting the versatility of macromolecular design in implementing next-generation redox-flow batteries.*

All-Organic redox-flow batteries are well positioned to offer low-cost, multi-hour electrochemical energy storage at large scale in line with targets for grid modernization.[1–6] During flow-battery operation, solutions of redox-active organic molecules (ROMs) in a non-aqueous electrolyte are circulated through the negative and positive electrode compartments of an electrochemical cell. These compartments are electronically isolated from each other by a separator or ion-conducting membrane.[7,8] In order to maximize cycle-life and efficiency, it is imperative to block ROMs from migrating between electrode compartments during cycling while also maintaining facile transport of the working ion.[9]

Here we show how this is achieved through macromolecular design principles advanced and applied to ROMs and ion-selective membranes derived from polymers of intrinsic microporosity (PIMs) (Figure 1). In contrast with traditional mesoporous battery separators, membranes derived from PIMs feature permanent micropores that in principle allow working-ion conduction while blocking the crossover of larger active-materials.[10–15] Indeed, we found that the effective diffusion coefficient (D_{eff}) for small-molecule ROMs (e.g., **1a**) through PIM-1 membranes decreased 40-fold compared to a Celgard separator with $\approx$20 nm pores. Additional gains in blocking ability (470-fold) were obtained by chemically cross-linking PIM-1 membranes, which restricted pore swelling in electrolyte. While these gains alone are impressive, we hypothesized that simply increasing the effective size of the ROM (e.g., through oligomerization) would provide active-materials that were larger than the PIM membrane's pore-size exclusion limit and thereby enable active-material blocking through a size-sieving mechanism. Indeed, by slightly increasing the molecular dimensions from 8.8 to 12.3 Å through oligomerization (Figure 2), D_{eff} fell below our experimental limit of quantification, with an estimated upper-bound of 3.4×10^{-11} cm^2 s^{-1}. Despite this $>$9000-fold improvement in membrane blocking ability relative to Celgard, PIM-1 membranes retained high ionic conductivities of at least 0.4 mS cm^{-1} (compared to 2.2 mS cm^{-1} for Celgard). Furthermore, we found that sieving oligomeric organic active materials (RAOs) by size with PIM membranes was general to different ROM chemistries (e.g., **3b** and **3c**) in a variety of battery electrolytes (e.g., ACN, PC, DME, etc.), showcasing the generality of our approach.

Breaking with convention, the advances reported here provide an important counterpoint to: 1) single-component electrodes paired with ceramic membranes, which are expensive and difficult to scale;[16] 2) thick macroporous separators paired with mixed-electrode formulations (i.e., anolytes and catholytes present in both electrode compartments), which lead to Coulombic inefficiencies and short cycle-life;[17,18] and 3) mesoporous separators paired with concentrated solutions of redox-active polymers (RAPs), which are difficult to pump

[*] S. E. Doris
Department of Chemistry, 419 Latimer Hall
University of California, Berkeley
Berkeley, CA 94720 (USA)
Dr. A. L. Ward, Dr. A. Baskin, Dr. P. D. Frischmann,
Dr. D. Prendergast, Dr. B. A. Helms
Joint Center for Energy Storage Research
Lawrence Berkeley National Laboratory
1 Cyclotron Road, Berkeley, CA 94720 (USA)
E-mail: bahelms@lbl.gov
Dr. N. Gavvalapalli, Dr. E. Chénard, Prof. J. S. Moore
Joint Center for Energy Storage Research
University of Illinois at Urbana-Champaign
505 South Matthews Avenue, Urbana, IL 61801 (USA)
Dr. C. S. Sevov
Joint Center for Energy Storage Research, University of Michigan
930 North University Avenue, Ann Arbor, MI 48109 (USA)
Dr. D. Prendergast, Dr. B. A. Helms
The Molecular Foundry, Lawrence Berkeley National Laboratory
1 Cyclotron Road, Berkeley, CA 94720 (USA)
Supporting information and the ORCID identification number(s) for the author(s) of this article can be found under http://dx.doi.org/10.1002/anie.201610582.

through electrochemical cells at high molecular weight and at all states-of-charge.[19–23] Our strategy to implement RAOs, as opposed to RAPs, should also serve to retain the facile charge transfer kinetics that are characteristic of ROMs, which is essential for power quality and high active-material utilization.[24]

To quantitatively inform the critical size regime for ROM-blocking by a size-selective polymer membrane, we designed a series of structurally minimal viologen-based ROMs and RAOs (**1a**–**3a**, Figure 1) and studied their solvated structures

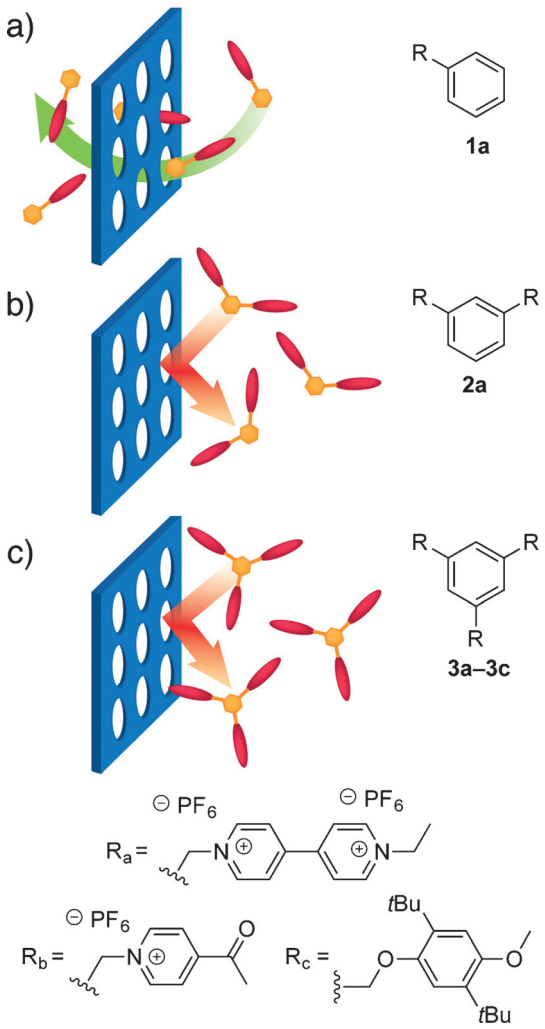

Figure 1. Macromolecular design strategies for preventing active-material crossover in all-organic redox-flow batteries: a) Small-molecule redox-active organic molecules (ROMs) pass through microporous membranes; b) and c) larger redox-active oligomers (RAOs) are blocked from passing through the membrane by a size-sieving mechanism.

computationally in acetonitrile (ACN) using a combination of ab initio quantum mechanical studies and classical molecular dynamics simulations (see the Supporting Information (SI), Figures S1–S6, Tables S1, S2). We were interested in understanding active-material solvation at different states of charge (SOCs), as the solvation will determine the effective size of each molecule and changes in solvation may affect the crossover behavior during cell cycling. For each RAO, we calculated the average number of ACN molecules as a function of distance from the molecule's Van der Waals surface (Figure 2) and found that the RAO solvation shells do not change significantly at different SOCs. This implies that membranes that are blocking to active-materials at one SOC will also block their crossover as the battery is cycled and the SOC changes. Furthermore, ACN molecules and PF_6^- counter-ions in the solvation shell are only weakly associated with the RAOs, and the solvation of RAOs in ACN does not lead to significant changes in conformation with respect to isolated geometries (Figures S5, S6). Therefore, the hydrodynamic radii and associated volumes of RAOs were computed from quantum mechanical calculations of isolated clusters. Characteristic sizes for viologen monomer (**1a**), dimer (**2a**) and trimer (**3a**) were 8.8, 12.3, and 16.8 Å, respectively, suggesting that polymer membranes with pore dimensions below 1.2 nm are likely to block the viologen dimer and trimer while considerably smaller pores would be required to sieve the monomer.

To validate the theoretical predictions of a critical size-regime for ROM-blocking, we synthesized **1a** (84%), **2a** (80%), and **3a** (69%) by a simple displacement reaction involving *N*-ethyl-4,4′-bipyridinium hexafluorophosphate and benzyl bromide, 1,3-bis(bromomethyl)benzene, and 1,3,5-tris(bromomethyl)benzene, respectively. Cyclic voltammetry of each compound showed that **1a**, **2a**, and **3a** are reversibly reduced at −0.75 V vs. Ag/Ag^+ (Figure S7, Table S3). This low reduction potential along with the high solubility of each species in ACN is promising for their use as energy dense anolytes in all-organic redox-flow batteries.[1] The crossover behavior for each RAO/membrane pairing was quantified by measuring the effective diffusion coefficient (D_{eff}) of each RAO through different membranes (Figures 3 and S8, S9, Tables S4, S5, see SI for details). Membrane blocking ability was quantified by comparing each RAO's diffusion coefficient through the membrane (D_{eff}) to its diffusion coefficient through solution (D_{sol}). For the non-selective Celgard membrane, high values for D_{eff}—$(5.4 \pm 0.4) \times 10^{-7}$, $(3.1 \pm 0.3) \times 10^{-7}$, and $(2.2 \pm 0.2) \times 10^{-7}$ $cm^2 s^{-1}$ for **1a**, **2a**, and **3a**, respectively—were measured. These D_{eff} are only 30-fold lower than D_{sol} for each species, indicating that the blocking ability of Celgard is equally poor for **1a**, **2a**, and **3a**. PIM-1 membranes, which feature nanometer-sized pores, significantly outperformed Celgard, with **1a**, **2a**, and **3a** diffusing through the membrane 1280, 11 600, and 32 900-fold slower, respectively, than through solution (Figure 3b). This dramatic improvement in membrane blocking-ability upon reducing the pore size from approximately 20 nm to less than 1 nm, along with the improved membrane blocking ability for larger RAOs, is indicative of size-selective transport of the active materials. However, our theoretical calculations of the sizes of **2a** and **3a** imply that both should be completely blocked by PIM-1 membranes. We hypothesized that swelling of the PIM-1 membranes in electrolyte increases the average pore size above the 0.9 nm pores present in dry membranes,[25] thus allowing some crossover of the larger RAOs.

By cross-linking PIM-1, the degree of swelling is controllable, and the membrane pore size is further constricted.

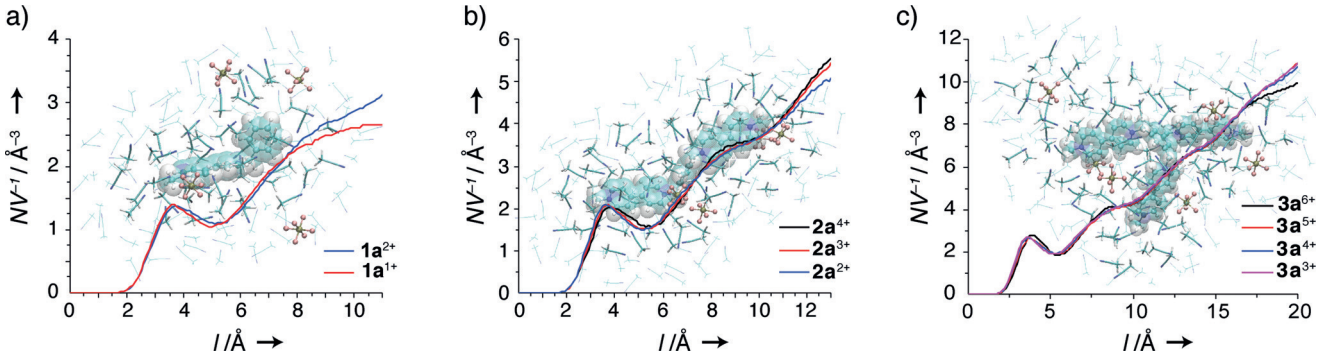

Figure 2. Computed solvation structures of a) **1a**, b) **2a**, and c) **3a** for different SOCs. The density of ACN molecules (NV^{-1}) as a function of distance (l) from each molecule's Van der Waals surface does not vary dramatically at different SOCs. Characteristic sizes of 8.8, 12.3, and 16.8 Å for **1a**, **2a**, and **3a**, respectively, were calculated from quantum mechanical calculations of isolated clusters with similar structures to the solvated clusters.

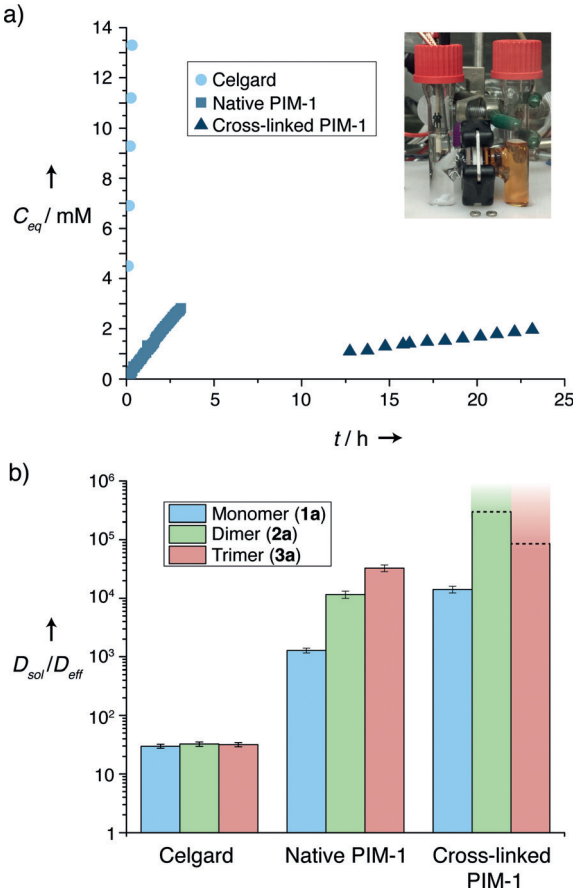

Figure 3. a) Equivalent concentration (C_{eq}) of **1a** in the permeate compartment as a function of time (t) for Celgard, native PIM-1, and cross-linked PIM-1 membranes. Inset: Picture of the crossover cell used to measure D_{eff}. b) Membrane blocking ability for each membrane paired with **1a**–**3a**. D_{sol}/D_{eff} describes how much slower the molecule diffuses through the membrane than through solution. The diffusion of **2a** and **3a** through cross-linked PIM-1 membranes was slower than the lower limit of quantification, so the minimum possible value of D_{sol}/D_{eff} is indicated by dashed lines.

Cross-linking was accomplished by casting solutions of PIM-1 containing the cross-linking agent 2,6-bis(4-azidobenzylidene)cyclohexanone. Upon heating the membranes, the azide groups of the cross-linking agent are converted to reactive nitrenes, which insert into C–H bonds on the polymer and cross-link the membranes (Figure S10).[11,26] Cross-linked PIM-1 membranes exhibited the best active-species blocking ability observed by any porous membrane platform to date, with **1a** diffusing through the membrane 14200-fold slower than through solution, and **2a** and **3a** diffusing slower than the limit of quantification (297000 and 85000-fold slower, respectively, than through solution). This unprecedented 9000-fold improvement in blocking ability for **2a** (with respect to Celgard) came at minimal cost to ionic conductivity, with cross-linked PIM-1 membranes only 5-fold less conductive than Celgard (0.4 vs. 2.2 mS cm^{-1}, Figures S11, S12).

To demonstrate that oligomerization is a generalizable approach to blocking ROM crossover in all-organic non-aqueous redox-flow batteries, we synthesized trimeric RAOs based on acylpyridinium hexafluorophosphate (**3b**, 89%) and DB3 (**3c**, 90%) redox-active pendant groups. Monomeric forms of these RAOs have been identified as promising candidates for non-aqueous redox-flow batteries, although their crossover through the battery membrane remains an issue.[2,3,27] Consistent with these reports, cyclic voltammetry showed evidence for reversible reduction of **3b** at −1.40 V vs. Ag/Ag$^+$ in 0.1 M TBAPF$_6$/propylene carbonate (PC). Likewise, **3c** underwent reversible oxidation at 0.56 V vs. Ag/Ag$^+$ in 0.1 M TBAPF$_6$/dimethoxyethane (DME). Both **3b** and **3c** were blocked by cross-linked PIM-1 membranes, with **3b** diffusing through the membrane slower than the lower limit of quantification of 1.0×10^{-11} cm^{2}s^{-1} and **3c** diffusing through the membrane with $D_{eff}=(8.1\pm0.7)\times10^{-10}$ cm^{2}s^{-1} (Figure 4). This corresponds to 26000 and 460-fold diminution in the crossover rate for **3b** and **3c**, respectively, when compared to their diffusion through non-selective mesoporous separators. Clearly, oligomerization provides a straightforward path to preparing a wide variety of RAOs that are effectively blocked by microporous polymer membranes.

Macromolecular design of both membranes and active-species is a powerful approach for solving the crossover problem in all-organic redox-flow batteries. Here we showed how computational chemistry informs the design of ROM oligomers, or RAOs, and that by pairing RAOs with RAO-

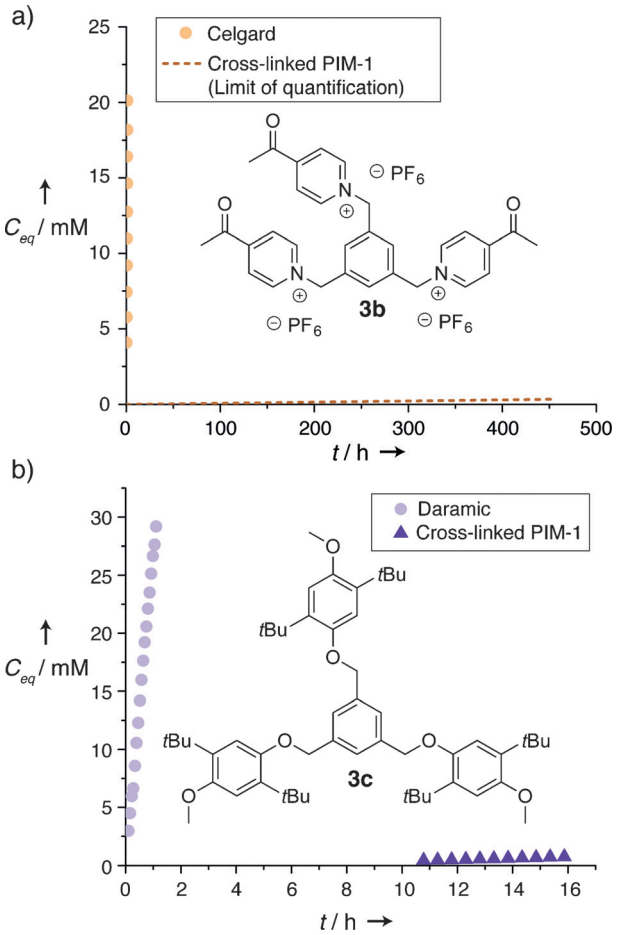

Figure 4. Equivalent RAO concentration (C_{eq}) in the permeate compartment as a function of time (t) for a) **3b** and b) **3c** paired with non-selective mesoporous and cross-linked PIM-1 membranes. The concentration of **3b** never reached the lower limit of quantification when paired with cross-linked PIM-1 (indicated by a dashed line), which is indicative of a size-sieving mechanism.

blocking microporous PIM membranes, active-material crossover is reduced by nearly four orders of magnitude with respect to commercially available battery separators with negligible decreases in ionic conductivity. ROM oligomerization was demonstrated for several redox-active motifs, including those that serve as either negative or positive electrode materials in redox-flow batteries. In all cases, RAO crossover was effectively blocked in a variety of battery solvents, including ACN, PC, and DME. These promising results point the way forward towards the design of new classes of RAOs and membranes for all-organic redox-flow batteries, along with their incorporation in next-generation redox-flow battery prototypes.

Experimental Section

Materials and methods, synthetic details, characterization, and membrane preparation are all described in the SI. All membranes were soaked in electrolyte (0.1 M $LiPF_6$ in ACN for **1a**–**3a**, 0.1 M $TBAPF_6$ in PC for **3b**, or 0.1 M $TBAPF_6$ in DME for **3c**) for at least 12 h before use. To allow comparison of membranes with different thicknesses, equivalent concentration (C_{eq}) refers to the concentration of ROM or RAO that would be observed with a 10 μm membrane and $C_0 = 0.1$ M (raw data can be found in the SI).

Acknowledgements

We thank C. Li and L. Maserati for samples of PIM-1 and D. Loudermilk (UIUC School of Chemical Sciences Graphic Services Facility) for assistance in the preparation of Figure 1. A.L.W., A.B., P.D.F., N.G., E.C., C.S.S., D.P., J.S.M., and B.A.H. were supported by the Joint Center for Energy Storage Research, an Energy Innovation Hub funded by the U.S. Department of Energy, Office of Science, Office of Basic Energy Sciences. S.E.D. was supported by the Department of Defense through the National Defense Science and Engineering Graduate Fellowship program. Portions of this work, including polymer synthesis and characterization, crossover measurements, and electrochemical experiments were carried out as user projects at the Molecular Foundry, which is supported by the Office of Science, Office of Basic Energy Sciences of the U.S. Department of Energy under contract no. DE-AC02-05CH11231. The computational portion of this work was supported by a user project at the Molecular Foundry and its computer cluster (Vulcan), managed by the High Performance Computing Services Group at Lawrence Berkeley National Laboratory (LBNL), and by the computing resources of the National Energy Research Scientific Computing Center, LBNL, both of which are supported by the Office of Science of the U.S. Department of Energy under the same contract.

Conflict of interest

The authors declare no conflict of interest.

Keywords: energy storage · macromolecular chemistry · membranes · polymers · redox-flow batteries

How to cite: *Angew. Chem. Int. Ed.* **2017**, *56*, 1595–1599
Angew. Chem. **2017**, *129*, 1617–1621

[1] R. M. Darling, K. G. Gallagher, J. A. Kowalski, S. Ha, F. R. Brushett, *Energy Environ. Sci.* **2014**, *7*, 3459.
[2] F. R. Brushett, J. T. Vaughey, A. N. Jansen, *Adv. Energy Mater.* **2012**, *2*, 1390.
[3] C. S. Sevov, R. E. M. Brooner, E. Chénard, R. S. Assary, J. S. Moore, J. Rodríguez-López, M. S. Sanford, *J. Am. Chem. Soc.* **2015**, *137*, 14465.
[4] B. Dunn, H. Kamath, J.-M. Tarascon, *Science* **2011**, *334*, 928.
[5] W. Wang, Q. Luo, B. Li, X. Wei, L. Li, Z. Yang, *Adv. Funct. Mater.* **2013**, *23*, 970.
[6] J. Noack, N. Roznyatovskaya, T. Herr, P. Fischer, *Angew. Chem. Int. Ed.* **2015**, *54*, 9776; *Angew. Chem.* **2015**, *127*, 9912.
[7] P. Arora, Z. Zhang, *Chem. Rev.* **2004**, *104*, 4419.
[8] S.-H. Shin, S.-H. Yun, S.-H. Moon, *RSC Adv.* **2013**, *3*, 9095.
[9] R. M. Darling, K. G. Gallagher, W. Xie, L. Su, F. R. Brushett, *J. Electrochem. Soc.* **2016**, *163*, A5029.
[10] C. Li, A. L. Ward, S. E. Doris, T. A. Pascal, D. Prendergast, B. A. Helms, *Nano Lett.* **2015**, *15*, 5724.

[11] S. E. Doris, A. L. Ward, P. D. Frischmann, L. Li, B. A. Helms, *J. Mater. Chem. A* **2016**, *4*, 16946.
[12] N. B. McKeown, P. M. Budd, *Chem. Soc. Rev.* **2006**, *35*, 675.
[13] P. M. Budd, B. S. Ghanem, S. Makhseed, N. B. McKeown, K. J. Msayib, C. E. Tattershall, *Chem. Commun.* **2004**, 230.
[14] N. B. McKeown, P. M. Budd, *Macromolecules* **2010**, *43*, 5163.
[15] P. Marchetti, M. F. J. Solomon, G. Szekely, A. G. Livingston, *Chem. Rev.* **2014**, *114*, 10735.
[16] P. Knauth, *Solid State Ionics* **2009**, *180*, 911.
[17] W. Duan, R. S. Vemuri, J. D. Milshtein, S. Laramie, R. D. Dmello, J. Huang, L. Zhang, D. Hu, M. Vijayakumar, W. Wang, J. Liu, R. M. Darling, L. Thompson, K. Smith, J. S. Moore, F. R. Brushett, X. Wei, *J. Mater. Chem. A* **2016**, *4*, 5448.
[18] X. Wei, W. Xu, J. Huang, L. Zhang, E. Walter, C. Lawrence, M. Vijayakumar, W. A. Henderson, T. Liu, L. Cosimbescu, B. Li, V. Sprenkle, W. Wang, *Angew. Chem. Int. Ed.* **2015**, *54*, 8684; *Angew. Chem.* **2015**, *127*, 8808.
[19] G. Nagarjuna, J. Hui, K. J. Cheng, T. Lichtenstein, M. Shen, J. S. Moore, J. Rodríguez-López, *J. Am. Chem. Soc.* **2014**, *136*, 16309.
[20] M. Burgess, J. S. Moore, J. Rodríguez-López, *Acc. Chem. Res.* **2016**, *49*, 2649.
[21] E. C. Montoto, G. Nagarjuna, J. Hui, M. Burgess, N. M. Sekerak, K. Hernández-Burgos, T.-S. Wei, M. Kneer, J. Grolman, K. J. Cheng, J. A. Lewis, J. S. Moore, J. Rodríguez-López, *J. Am. Chem. Soc.* **2016**, *138*, 13230.
[22] T. Janoschka, N. Martin, U. Martin, C. Friebe, S. Morgenstern, H. Hiller, M. D. Hager, U. S. Schubert, *Nature* **2015**, *527*, 78.
[23] J. Winsberg, T. Hagemann, S. Muench, C. Friebe, B. Häupler, T. Janoschka, S. Morgenstern, M. D. Hager, U. S. Schubert, *Chem. Mater.* **2016**, *28*, 3401.
[24] M. Burgess, E. Chénard, K. Hernandez-Burgos, G. Nagarjuna, R. S. Assary, J. Hui, J. S. Moore, J. Rodríguez-López, *Chem. Mater.* **2016**, *28*, 7362.
[25] C. L. Staiger, S. J. Pas, A. J. Hill, C. J. Cornelius, *Chem. Mater.* **2008**, *20*, 2606.
[26] N. Du, M. M. Dal-Cin, I. Pinnau, A. Nicalek, G. P. Robertson, M. D. Guiver, *Macromol. Rapid Commun.* **2011**, *32*, 631.
[27] J. Huang, L. Cheng, R. S. Assary, P. Wang, Z. Xue, A. K. Burrell, L. A. Curtiss, L. Zhang, *Adv. Energy Mater.* **2015**, *5*, 1401782.

Manuscript received: October 28, 2016
Final Article published: January 10, 2017

